



Journal of Coordination Chemistry

Publication details, including instructions for authors and subscription information:

<http://www.tandfonline.com/loi/gcoo20>

Structures, DNA binding, DNA cleavage, and antitumor investigations of a series of molybdenum(VI) complexes with some N(4) methyl and ethyl thiosemicarbazone ligands

Mouayed A. Hussein^a, Teoh S. Guan^a, Rosenani A. Haque^a, Mohamed B. Khadeer Ahamed^b & Amin M.S. Abdul Majid^b

^a School of Chemical Science, Universiti Sains Malaysia, Minden, Malaysia

^b EMAN Research and Testing Laboratory, School of Pharmaceutical Sciences, Universiti Sains Malaysia, Minden, Malaysia

Accepted author version posted online: 13 Feb 2014. Published online: 20 Mar 2014.



CrossMark

[Click for updates](#)

To cite this article: Mouayed A. Hussein, Teoh S. Guan, Rosenani A. Haque, Mohamed B. Khadeer Ahamed & Amin M.S. Abdul Majid (2014) Structures, DNA binding, DNA cleavage, and antitumor investigations of a series of molybdenum(VI) complexes with some N(4) methyl and ethyl thiosemicarbazone ligands, *Journal of Coordination Chemistry*, 67:4, 714-727, DOI: [10.1080/00958972.2014.893430](https://doi.org/10.1080/00958972.2014.893430)

To link to this article: <http://dx.doi.org/10.1080/00958972.2014.893430>

PLEASE SCROLL DOWN FOR ARTICLE

Taylor & Francis makes every effort to ensure the accuracy of all the information (the "Content") contained in the publications on our platform. However, Taylor & Francis, our agents, and our licensors make no representations or warranties whatsoever as to the accuracy, completeness, or suitability for any purpose of the Content. Any opinions and views expressed in this publication are the opinions and views of the authors, and are not the views of or endorsed by Taylor & Francis. The accuracy of the Content should not be relied upon and should be independently verified with primary sources of information. Taylor and Francis shall not be liable for any losses, actions, claims, proceedings, demands, costs, expenses, damages, and other liabilities whatsoever or howsoever caused arising directly or indirectly in connection with, in relation to or arising out of the use of the Content.

This article may be used for research, teaching, and private study purposes. Any substantial or systematic reproduction, redistribution, reselling, loan, sub-licensing, systematic supply, or distribution in any form to anyone is expressly forbidden. Terms & Conditions of access and use can be found at <http://www.tandfonline.com/page/terms-and-conditions>

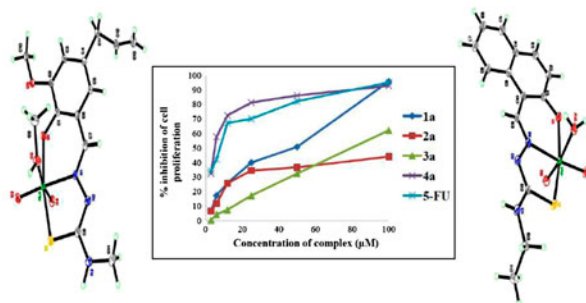
Structures, DNA binding, DNA cleavage, and antitumor investigations of a series of molybdenum(VI) complexes with some N(4) methyl and ethyl thiosemicarbazone ligands

MOUAYED A. HUSSEIN†, TEOH S. GUAN*†, ROSENANI A. HAQUE†,
MOHAMED B. KHADEER AHAMED‡ and AMIN M.S. ABDUL MAJID‡

†School of Chemical Science, Universiti Sains Malaysia, Minden, Malaysia

‡EMAN Research and Testing Laboratory, School of Pharmaceutical Sciences, Universiti Sains Malaysia, Minden, Malaysia

(Received 13 September 2013; accepted 15 January 2014)



Four dioxomolybdenum(VI) complexes were synthesized by reaction of $[\text{MoO}_2(\text{aac})_2]$ with thiosemicarbazones derived from 5-allyl-2-hydroxy-3-methoxybenzaldehyde (**1**), 2-hydroxynaphthaldehyde (**2**), 2,3-dihydroxybenzaldehyde (**3**), or 5-tert-butyl-2-hydroxybenzaldehyde (**4**). The ligands were coordinated to molybdenum as tridentate ONS donors. X-ray crystallography showed that the distorted octahedral coordination of molybdenum is completed by methanol (D) in **1a**, **3a**, and **4a** or H_2O in **2a**. The molecular structures of **1**, **3**, and **4**, and the complexes were determined by single-crystal X-ray crystallography. Binding of the ligand and complexes with calf thymus DNA were investigated by UV, fluorescence titrations, and viscosity measurements. Gel electrophoresis revealed that all the complexes can cleave pBR322 plasmid DNA. The cytotoxic properties of the complexes against human colorectal (HCT 116) cell line showed strong antiproliferative activities in relative order **4a** > **3a** > **1a** > **2a** with IC_{50} values of 1.6, 4.0, 4.8, and 6.7 μM , respectively. The complexes exhibited more activity than the standard reference drug, 5-fluorouracil (IC_{50} 7.3 μM). These studies show that dioxomolybdenum(VI) complexes have potential use in chemotherapy.

Keywords: Thiosemicarbazone; Molybdenum(VI) complexes; X-ray crystal structure; DNA binding; DNA cleavage; Antiproliferative activity

*Corresponding author. Email: sgteoh@usm.my

1. Introduction

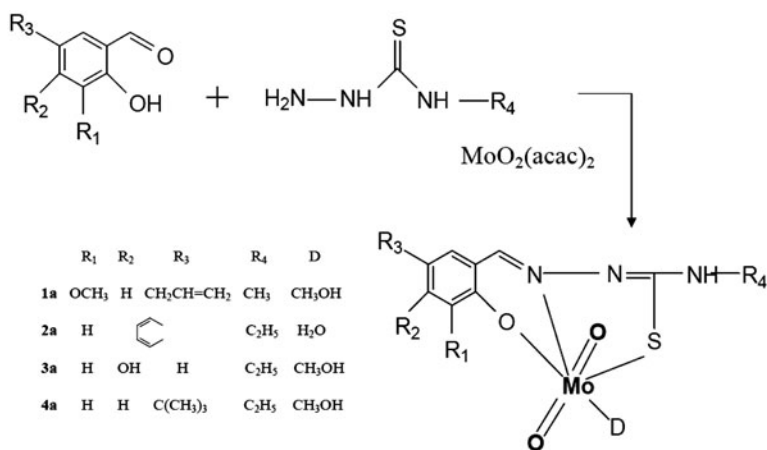
Thiosemicarbazones have applications in biology and medicine [1, 2] with antifungal, antibacterial, and anticancer activities [3, 4]. The biological activity is a result of their ability to chelate with transition metal ions that bond through oxygen, nitrogen, and sulfur (ONS) [5] or sulfur and two nitrogens [6]. Because thiosemicarbazone complexes are generally more active than free ligands, the biological and pharmaceutical activities of ONS tridentate systems and their metal complexes have received interest [7–9].

The coordination chemistry of molybdenum(VI) has biochemical significance [10–12]; ONS ligands around Mo(VI) in oxotransferase enzymes have led to interest in these types of complexes and oxotransfer ability. Such complexes can serve as models that mimic oxotransferase molybdoenzymes [13–15]. Structural studies have shown that thiosemicarbazone derivatives containing phenolic oxygen and acting as tridentate ONS donors coordinate strongly [16–18]. In the present study, we report the synthesis and characterization of *cis*-dioxomolybdenum(VI) complexes with 4-methyl (or ethyl) thiosemicarbazones shown in scheme 1. The complexes were tested for their calf thymus DNA (CT DNA) binding, cleavage of pBR322 plasmid DNA, and antiproliferative property against human colorectal (HCT 116) cell line.

2. Experimental

2.1. Synthesis of ligands

The ligands were prepared by following a general procedure in which a solution of corresponding aldehyde in ethanol (20 mL) was added to an ethanolic solution (20 mL) of 4-methyl-3-thiosemicarbazide (4.75 mM) or 4-ethyl-3-thiosemicarbazide (4.19 mM). The mixture was refluxed with stirring for 2 h. The product was filtered, washed with ethanol, and air-dried. Crystals for **1** were obtained by slow evaporation of DMF solution at room temperature. Crystals for **3** and **4** were obtained by slow evaporation of ethanol solution at room temperature.



Scheme 1. General synthetic procedure of ligands and complexes.

(1) M.p.: 176–178 °C (1.09 g, 83%). Anal. Calcd for $C_{13}H_{16}N_3O_2S$: C, 55.83; H, 5.72; N, 15.03. Found: C, 55.77; H, 5.74; N, 14.96%. IR(KBr) ($\nu_{\max}/\text{cm}^{-1}$): 3317 (s, NH), 1609 (m, C=N), 1550 (s, $C_{\text{aro}}\text{O}$), 1275 (s, C=S). ^1H NMR (DMSO- d_6 , ppm): 3.01 (CH_3), 3.30 ($\text{CH}_2\text{-Ph}$), 3.79 (O- CH_3), 5.02 (=CH), 6.02 ($\text{CH}_2=$), 6.78–7.34 (H-aromatic), 8.37 (CS-NH), 9.09 (CH=N), 11.40 (N-NH). ^{13}C NMR (DMSO- d_6 , ppm): 30.83 (CH_3), 55.85 (O- CH_3), 113.16 ($\text{CH}_2\text{-Ph}$), 115.46 ($\text{H}_2\text{C=}$), 117.49–144.28 (C-aromatic), 147.88 (C=N), 177.52 (C=S).

(2) M.p.: 213–215 °C (1.03 g, 90%). Anal. Calcd for $C_{14}H_{15}N_3\text{OS}$: C, 61.45; H, 5.48; N, 15.36. Found: C, 61.33; H, 5.46; N, 15.35%. IR(KBr) ($\nu_{\max}/\text{cm}^{-1}$): 3405 (m, NH), 3149 (m, OH), 1600–1612 (m, C=N-N-C), 1537 (s, $C_{\text{aro}}\text{O}$), 1264 (m, C=S). ^1H NMR (DMSO- d_6 , ppm): 1.17 (CH_3), 3.61 (CH_2), 7.20–7.89, 8.418 (H-aromatic), 8.37 (CS-NH), 9.06 (CH=N). ^{13}C NMR (DMSO- d_6 , ppm): 14.49 (CH_3), 30.62 (CH_2), 109.77–142.61 (C-aromatic), 156.30 (C=N), 176.42 (C=S).

(3) M.p.: 201–203 °C (0.78 g, 78%). Anal. Calcd for $C_{10}H_{13}N_3O_2S$: C, 50.14; H, 5.43; N, 17.55. Found: C, 48.01; H, 5.74; N, 18.79%. IR(KBr) ($\nu_{\max}/\text{cm}^{-1}$): 3399 (s, NH), 3146 (m, OH), 1612 (m, C=N). ^1H NMR (DMSO- d_6 , ppm): 1.08 (CH_3), 3.54 (CH_2), 6.27–7.70 (H-aromatic), 8.25 (CS-NH), 8.30 (CH=N), 9.76, 9.79 (OH), 11.14 (N-NH). ^{13}C NMR (DMSO- d_6 , ppm): 14.68 (CH_3), 37.64 (CH_2), 102.28–157.87 (C-aromatic), 160.34 (C=N), 177.31 (C=S).

(4) M.p.: 210–212 °C (1.05 g, 90%). Anal. Calcd for $C_{14}H_{21}N_3\text{OS}$: C, 60.12; H, 7.51; N, 15.03. Found: C, 59.72; H, 7.97; N, 15.04%. IR(KBr) ($\nu_{\max}/\text{cm}^{-1}$): 3352 (s, NH), 3275 (m, OH), 1603 (m, C=N), 1545 (s, $C_{\text{aro}}\text{O}$). ^1H NMR (DMSO- d_6 , ppm): 1.16 (CH_3), 1.27 { $\text{C}(\text{CH}_3)_3$ }, 3.60 (CH_2), 6.80–7.73 (H-aromatic), 8.34 (CS-NH), 8.37 (CH=N), 9.69 (OH), 11.30 (N-NH). ^{13}C NMR (DMSO- d_6 , ppm): 14.60 (CH_3), 31.31 {(CH_3) $_3$ }, 33.82 { $\underline{\text{C}}(\text{CH}_3$)}, 38.30 (CH_2), 115.71–141.49 (C-aromatic), 154.24 (C=N), 176.43 (C=S).

2.2. Synthesis of complexes

Equimolar methanolic or ethanolic solutions (25 mL) of $\text{MoO}_2(\text{acac})_2$ and the corresponding ligand were refluxed for 2 h, and then filtered. Slow evaporation of a solvent at room temperature gives a crystalline product.

Complex **2a** was prepared by the following procedure in which a solution of $\text{MoO}_2(\text{acac})_2$ (0.119 g, 0.365 mM) in ethanol (25 mL) was added to a solution of **2** (0.1 g, 0.365 mM) in ethanol (25 mL). The resulting red solution was refluxed for 2 h and then filtered. The filtrate was left to stand at room temperature for one week to obtain purple block-shaped crystals.

(1a) M.p.: 167–169 °C (0.11 g, 71%). Anal. Calcd for $C_{14}H_{19}\text{MoN}_3\text{O}_5\text{S}$: C, 38.41; H, 4.34; N, 9.60; Mo, 21.94. Found: C, 37.08; H, 3.37; N, 9.79; Mo, 21.77%. IR(KBr) ($\nu_{\max}/\text{cm}^{-1}$): 3324 (m, NH), 3437 (m, OH), 1589 (m, C=N), 1568 (m, $C_{\text{aro}}\text{O}$), 1268 (s, C-S), 932, 898 (s, Mo=O). ^1H NMR (DMSO- d_6 , ppm): 3.01 (CH_3), 2.86 (alcoholic- CH_3), 3.30 ($\text{CH}_2\text{-Ph}$), 3.79 (O- CH_3), 5.02 (=CH), 5.79 ($\text{CH}_2=$), 6.78, 7.34 (H-aromatic), 7.46 (alcoholic-OH), 8.37 (C-NH), 8.47 (CH=N); ^{13}C NMR (DMSO- d_6 , ppm): 30.83 (CH_3), 46.35 (alcoholic- CH_3), 55.85 (O- CH_3), 115.51 ($\text{CH}_2\text{-Ph}$), 115.93 (=CH), 117.37 ($\text{H}_2\text{C=}$), 120.26–147.05 (C-aromatic), 148.09 (C=N), 151.45 (C-S).

(2a) M.p.: 222–224 °C (0.11 g, 74%). Anal. Calcd for $C_{14}H_{15}\text{MoN}_3\text{O}_4\text{S}$: C, 40.25; H, 3.59; N, 10.06; Mo, 23.00. Found: C, 40.55; H, 2.81; N, 10.01; Mo, 22.96%. IR(KBr) ($\nu_{\max}/\text{cm}^{-1}$): 3333 (s, NH), 1591 (m, C=N), 1552 (m, $C_{\text{aro}}\text{O}$), 1281 (m, C-S), 938, 900 (s, Mo=O). ^1H NMR (DMSO- d_6 , ppm): 1.17 (CH_3), 3.35 (CH_2), 7.14, 7.45, 7.65, 7.89, 7.99,

8.28 (H-aromatic), 7.55 (H₂O), 8.31 (C–NH), 8.45 (CH=N); ¹³C NMR (DMSO-d₆, ppm): 14.47 (CH₃), 30.61 (CH₂), 112.16–142.93 (C-aromatic), 146.83 (C=N), 159.43 (C–S).

(3a) M.p.: 219–221 °C (0.14 g, 85%). Anal. Calcd for C₁₁H₁₅MoN₃O₅S: C, 33.22; H, 3.77; N, 10.57; Mo, 24.15. Found: C, 32.78; H, 3.0; N, 11.44; Mo, 24.11%. IR(KBr) ($\nu_{\max}/\text{cm}^{-1}$): 3379 (m, NH), 1592 (m, C=N), 1557 (m, C_{aro}O), 936, 897 (s, Mo=O). ¹H NMR (DMSO-d₆, ppm): 1.08 (CH₃), 3.16 (alcoholic-CH₃), 3.25 (CH₂), 6.20, 6.47, 7.41 (H-aromatic), 7.24 (alcoholic-OH), 8.25 (C–NH), 8.38 (CH=N) 10.45 (OH); ¹³C NMR (DMSO-d₆, ppm): 14.39 (CH₃), 38.19 (CH₂), 48.57 (alcoholic-CH₃), 102.28–134.86 (C-aromatic), 151.72 (C=N), 162.64 (C–S).

(4a) M.p.: 180–182 °C (0.14 g, 93%). Anal. Calcd for C₁₅H₂₃MoN₃O₄S: C, 41.15; H, 5.25; N, 9.60; Mo, 21.94. Found: C, 40.64; H, 4.97; N, 9.69; Mo, 21.81%. IR(KBr) ($\nu_{\max}/\text{cm}^{-1}$): 3440 (s, NH), 1589–1607 (m, C=N–N–C), 1557 (s, C_{aro}O), 936, 901 (s, Mo=O). ¹H NMR (DMSO-d₆, ppm): 1.16 (CH₃), 1.27 [(CH₃)₃], 3.16 (alcoholic-CH₃), 3.29 (CH₂), 6.79, 7.49, 7.59 (H-aromatic), 7.45 (alcoholic-OH), 8.31 (C–NH), 8.55 (CH=N); ¹³C NMR (DMSO-d₆, ppm): 14.35 (CH₃), 31.04 [(CH₃)₃], 31.24 [C(CH₃)₃], 33.77 (CH₂), 48.56 (alcoholic-CH₃), 117.22–143.34 (C-aromatic), 151.82 (C=N), 156.68 (C–S).

2.3. DNA binding and cleavage

The binding of complexes with CT DNA was investigated in 6.3 mM Tris–HCl/50 mM NaCl buffer (pH 7). The stock solution of DNA was prepared by dissolution of a suitable amount of DNA in 6.3 mM Tris–HCl/50 mM NaCl buffer (pH 7) at room temperature and stored in a refrigerator for 2 days. A solution of CT DNA in the buffer gave a UV absorbance ratio at 260 and 280 nm of ca. 1.9 : 1, indicating that the DNA was sufficiently free of protein. The DNA concentration was estimated by UV absorbance at 260 nm with a known molar absorption coefficient of 6600 M^{−1} cm^{−1} [19]. The UV–Vis spectra were scanned from 230 to 600 nm with a Tris/HCl buffer solution as reference.

Fluorescence emission assay was performed with the aforementioned method. The fluorescence spectra were scanned from 200 to 800 nm with a Tris/HCl buffer solution as reference.

Viscosity measurements were made with a Cannon–Manning Semi-Micro viscometer immersed in a thermostatic water bath at 37 °C. Flow times were measured manually with a digital stopwatch. The viscosity values were calculated from the observed flow time of DNA-containing solutions (t) corrected for that of the solvent mixture used (t_0), $\eta = t - t_0$. Viscosity data are presented as $(\eta/\eta_0)^{1/3}$ versus [complex]/[DNA], where η and η_0 are the viscosity of the complex in the presence of DNA and the viscosity of DNA alone, respectively [20].

The ability of the ligands and complexes to cleave pBR322 plasmid DNA was studied by agarose gel electrophoresis in Tris/EDTA buffer solution. The samples were incubated at 37 °C for 2 h, treated with loading dye, and electrophoresed for 1 h at 50 V on 1% agarose gel consisting of 12 lanes: lane 1, pBR322 DNA (0.025 μM); lane 2, DNA (0.025 μM) + sample (6 μM); lane 3, DNA (0.025 μM) + H₂O₂ (4.5 μM); lane 4, DNA (0.025 μM) + H₂O₂ (4.5 μM) + sample (1 μM); lane 5, DNA (0.025 μM) + H₂O₂ (4.5 μM) + sample (2 μM); lane 6, DNA (0.025 μM) + H₂O₂ (4.5 μM) + sample (3 μM); lane 7, DNA (0.025 μM) + H₂O₂ (4.5 μM) + sample (3.5 μM); lane 8, DNA (0.025 μM) + H₂O₂ (4.5 μM) + sample (4 μM); lane 9, DNA (0.025 μM) + H₂O₂ (4.5 μM) + sample (4.5 μM); lane 10, DNA (0.025 μM) + H₂O₂ (4.5 μM) + sample (5 μM); lane 11, DNA (0.025 μM) + H₂O₂ (4.5 μM) + sample (6 μM). The gel was then stained with ethidium bromide before being photographed under UV light.

2.4. Antiproliferative assay

2.4.1. Preparation of cell culture. HCT 116 cells were grown under optimum incubation conditions. Cells that reached 70–80% confluence were chosen for cell plating purposes. The old medium was replaced by aspiration. Then, the cells were washed with sterile PBS (pH 7.4) two to three times. The intact layer of attached cells was subjected to trypsinization. The cells were incubated at 37 °C in 5% CO₂ for 3–5 min. Then, the flasks containing the cells were gently tapped to aid in cell segregation and observed under inverted microscope (to confirm whether cell segregation was complete). Trypsin activity was inhibited by the addition of 5 mL of fresh complete media supplied with 10% fetal bovine serum. The cells were counted and diluted to obtain a final concentration of 2.5×10^5 cells/mL and inoculated into wells (100 μ L/well). Plates containing the cells were incubated at 37 °C with an internal atmosphere of 5% CO₂.

2.4.2. MTT assay. The cytotoxicity was evaluated with MTT assay [21] against HCT 116 cells. HCT 116 cells (1.5×10^5 cells/mL, 100 μ L/well) were seeded in a 96-well microtiter plate. The plate was incubated in a CO₂ incubator overnight to allow cell attachment. We added 100 μ L of test substance into each well containing the cells. The test substance was diluted with media into the desired concentrations from the stock. The plates were incubated at 37 °C with an internal atmosphere of 5% CO₂ for 72 h. After this treatment period, 20 μ L of MTT reagent was added into each well and the plates were incubated for 4 h. After this incubation period, 50 μ L of MTT lysis solution (DMSO) was added into the wells. The plates were further incubated for 5 min in a CO₂ incubator. Finally, the plates were read at 570 and 620 nm with the use of a standard ELISA microplate reader. Data were recorded and analyzed to assess the effects of test substance on cell viability. The percentage of growth inhibition was calculated from the optical density (OD) obtained from the MTT assay, or the 100th multiple of the subtracted OD value of the control and survived cells over the OD of the control cells.

3. Results and discussion

3.1. Chemistry

New dioxomolybdenum(VI) complexes were synthesized by reaction of [MoO₂(acac)₂] with substituted thiosemicarbazones. The ligands were prepared by condensation of thiosemicarbazone with salicylaldehyde derivatives [22]. The X-ray crystal structure shows distorted octahedral complexes, in which the complex surrounding the molecules consists of *cis*-MoO₂²⁺ core to which the doubly deprotonated tridentate ligand is meridionally bonded via the phenolate-oxygen, imine-nitrogen, and thiolate-sulfur. The sixth coordination site is occupied by CH₃OH or H₂O. All the ligands and complexes are air-stable and highly soluble in DMSO and DMF; the ligands and complexes are insoluble [23] and highly stable in aqueous solutions. ¹H NMR and UV spectra were recorded after preparation, 7 days, 30 days, 3 months, and 8 months, while kept at room temperature. All spectra confirmed the stability of the ligand and complexes in aqueous solutions.

3.2. Crystal and molecular structure

The crystal and molecular structures of the complexes were obtained by single-crystal X-ray diffraction. Crystal data of complexes are collected in table 1. The relevant bond distances and angles are collected in table 2.

In all the complexes, molybdenum has a distorted octahedral coordination. The Schiff base is bonded to *cis*-MoO₂²⁺ through phenolate oxygen O1, imine nitrogen N1, and thiolate sulfur S1; oxo O3 is *trans* to N1, whereas the other oxo {O2 in **2a**} lies *trans* to the D site, which is occupied by CH₃OH in **1a**, **3a**, and **4a** or H₂O in **2a**. The molecular structure of **2a** is depicted in figure 1. Despite the complex being prepared using ethanol (99%), H₂O occupies the D site. There are two significant differences in conformation geometries between **2a** and the other complexes, where CH₃OH occupies the D site. For **2a**, C13 from the N-ethyl group is *cis* to S1 and *trans* to N2, whereas for **3a** (figure 2) and **4a** C9 from N-ethyl is *trans* to S1 and *cis* to N2. For **1a**, C14 from N-methyl is *trans* to S1 and *cis* to N2. The stereochemistry is governed by the steric effect of the substituents in the thiosemicarbazone [24]. To increase stability due to better electron delocalization, in a chelated ring system resulting from coordination the metal coordinates with a suitable ligand for this purpose. Accordingly, **2a** coordinates with H₂O rather than CH₃OH. Substitution by water and methanol was determined using ¹H NMR and UV spectroscopy.

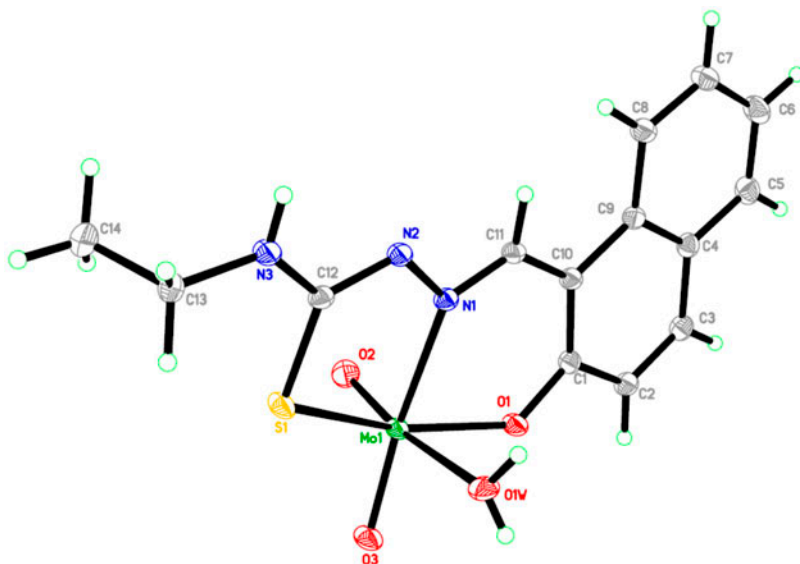
The Mo–O2 bond distances of 2.3613(14) and 2.3604(8) Å in **1a** and **4a**, respectively, are longer than that of 2.3389(16) Å in **3a**, showing the substituent effect of the aromatic ring and the repulsion between O3 and O4 oxo groups. The double bonds to molybdenum have bond distances ranging from 1.7141(12) to 1.7258(14) Å and 1.6953(13) to 1.6986(9) Å for Mo–O3 and Mo–O4, respectively. In **2a**, the Mo–O1W bond distance of 2.3208(13) Å exhibits strong bonding with MoO₂²⁺ compared with CH₃OH.

Table 1. Crystallographic data for **1a–4a**.

	1a	2a	3a	4a
Chemical formula	C ₁₄ H ₁₉ MoN ₃ O ₅ S	C ₁₄ H ₁₅ MoN ₃ O ₄ S	C ₁₁ H ₁₅ MoN ₃ O ₅ S	C ₁₅ H ₂₃ MoN ₃ O ₄ S
Formula weight	437.33	417.30	397.27	437.37
Crystal system	Triclinic	Triclinic	Triclinic	Monoclinic
Crystal description	Plate orange	Block purple	Needle brown	Block orange
Space group	<i>P</i> -1	<i>P</i> -1	<i>P</i> -1	<i>P</i> ₂ / <i>c</i>
<i>Unit cell dimensions</i>				
<i>a</i> (Å)	7.0017(1)	8.3956(1)	7.3557(1)	7.3552(1)
<i>b</i> (Å)	10.9150(2)	9.5796(1)	9.5561(2)	16.2793(3)
<i>c</i> (Å)	11.7132(2)	10.5286(1)	10.9126(2)	15.3487(3)
<i>α</i> (°)	76.564(1)	67.264(1)	95.558(1)	90
<i>β</i> (°)	78.085(1)	84.266(1)	109.129(1)	104.219(1)
<i>γ</i> (°)	89.197(1)	85.028(1)	92.071	90
Volume (Å ³)	851.36(3)	776.006(15)	719.42(2)	1781.51(5)
<i>Z</i>	2	2	2	4
<i>D</i> _{calcd} (g/cm ³)	1.706	1.786	1.834	1.631
Crystal size (mm)	0.05 × 0.19 × 0.41	0.11 × 0.19 × 0.35	0.08 × 0.09 × 0.44	0.13 × 0.19 × 0.58
Temperature (K)	100	100	100	100
Total data	19,993	20,471	19,563	25,336
Unique data	6219	5618	5214	6508
<i>R</i> _{int}	0.027	0.019	0.019	0.024
Observed data [<i>I</i> > 2σ(<i>I</i>)]	5682	5230	4844	6039
<i>R</i> ₁	0.0282	0.0222	0.0220	0.0213
<i>wR</i> ₂	0.0671	0.0588	0.0754	0.0518
<i>S</i>	1.11	1.05	1.22	1.04

Table 2. Selected bond distances (Å) and angles (°) for **1a–4a**.

	1a	2a	3a	4a
<i>Bond distances (Å)</i>				
Mo–S1	2.4268(5)	2.4337(4)	2.4243(6)	2.4417(3)
Mo–O1	1.9198(13)	1.9585(11)	1.9250(15)	1.9324(8)
Mo–O2	2.3613(14)	2.3208(13)*	2.3389(16)	2.3604(8)
Mo–O3	1.7258(14)	1.7141(12)	1.7206(15)	1.7120(8)
Mo–O4	1.6953(13)	1.6966(13)*	1.6973(16)	1.6986(9)
Mo–N1	2.2689(14)	2.2559(12)	2.2657(16)	2.2864(9)
S1–C8	1.761(2)	1.7423(14)*	1.757(2)	1.7555(4)
N2–C8	1.308(2)	1.3154(19)	1.312(3)	1.3437(15)
<i>Bond angles (°)</i>				
S1–Mo–O1	152.06(4)	153.49(3)	153.53(5)	155.58(2)
S1–Mo–O2	79.17(3)	81.37(3)*	82.62(4)	83.52(2)
S1–Mo–O3	89.49(5)	92.66(4)	89.51(5)	90.94(3)
S1–Mo–O4	98.80(5)	97.58(4)*	97.96(6)	95.06(3)
S1–Mo–N1	76.63(4)	76.84(3)	75.73(4)	75.62(2)
O1–Mo–O2	77.66(5)	79.26(5)	77.61(6)	80.60(3)
O1–Mo–O3	104.35(6)	102.67(5)	105.03(7)	104.90(4)
O1–Mo–O4	100.62(6)	98.72(6)	99.22(7)	98.52(4)
O1–Mo–N1	82.85(5)	81.59(4)	83.65(6)	82.59(3)
O2–Mo–O3	86.41(6)	82.87(5)	82.61(6)	81.67(3)
O2–Mo–O4	168.00(6)	170.98(5)	171.87(7)	173.21(4)
O2–Mo–N1	76.17(5)	78.18(4)	80.19(6)	76.05(3)
O3–Mo–O4	105.45(6)	106.14(6)	105.49(7)	105.01(4)
O3–Mo–N1	159.39(6)	159.47(5)	158.58(7)	155.04(4)
O4–Mo–N1	91.84(6)	92.84(5)	92.07(7)	97.17(4)

*For **2a**: O2 = O1W, O4 = O2.Figure 1. ORTEP diagram of **2a**.

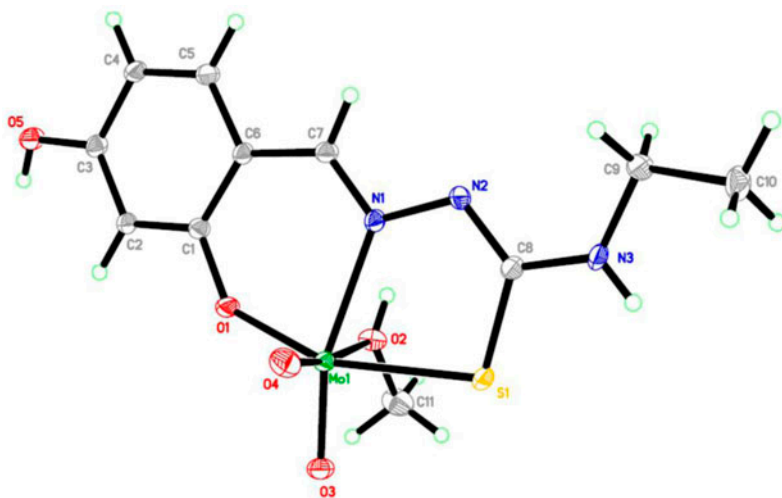


Figure 2. ORTEP diagram of **3a**.

3.3. Interaction with DNA

3.3.1. Electronic absorption studies. Electronic absorption spectroscopy is used to investigate the binding of compounds with DNA [25, 26]. Complexes can bind to DNA through covalent bonding [27] or non-covalent interactions such as intercalation, electrostatic, or groove binding [28]. Absorption spectroscopic studies were conducted on a Perkin Elmer, Lambda 35 spectrophotometer using a fixed concentration of ligand or complex (50 μM) with increasing amounts of DNA from 28.9 to 173.4 μM in 6.3 mM Tris-HCl/50 mM NaCl buffer (pH 7). Each addition was left for equilibrium at 25 $^{\circ}\text{C}$ for 10 min and scanned from 230 to 600 nm. The electronic absorption spectra (figure 3) showed one absorption for **1a** at 305 nm, which is attributed to $\pi-\pi^*$ transition. Complex **2a** showed three absorptions at 321 nm attributed to $\pi-\pi^*$ transition, and the 331 and 368 nm attributed to $n-\pi^*$ transitions. **3a** and **4a** showed two absorptions at 308 and 338 nm attributed to $\pi-\pi^*$ and $n-\pi^*$ transitions, respectively. All the ligands showed the same transitions as their complexes.

The $\pi-\pi^*$ absorptions were chosen to study the interaction of CT DNA with ligands and complexes. Increasing additions of DNA resulted in hypochromism in the absorption bands with no apparent shifts observed. This spectral behavior suggests intercalative binding to DNA [29].

The binding strengths of ligands and complexes to CT DNA were determined from the calculated binding constant (K_b) with the following equation [30]:

$$[\text{DNA}]/(\varepsilon_a - \varepsilon_f) = [\text{DNA}]/(\varepsilon_b - \varepsilon_f) + 1/K_b(\varepsilon_b - \varepsilon_f)$$

The absorption coefficients ε_a , ε_f and ε_b correspond to $A_{\text{abs}}/[\text{DNA}]$, the extinction coefficient for the free complex, and the extinction coefficient for the complex in fully bound form, respectively. A plot of $[\text{DNA}]/(\varepsilon_a - \varepsilon_f)$ versus $[\text{DNA}]$ yields a slope of $1/(\varepsilon_a - \varepsilon_f)$ and intercept of $1/K_b (\varepsilon_b - \varepsilon_f)$. The binding constants (table 3) suggest that the complexes exhibit strong interactions compared with the ligands. The highest K_b of $3.698 \times 10^6 \text{ M}^{-1}$ was observed for **4a**, whereas the lowest K_b of $1.033 \times 10^5 \text{ M}^{-1}$ was observed for **2a**. By

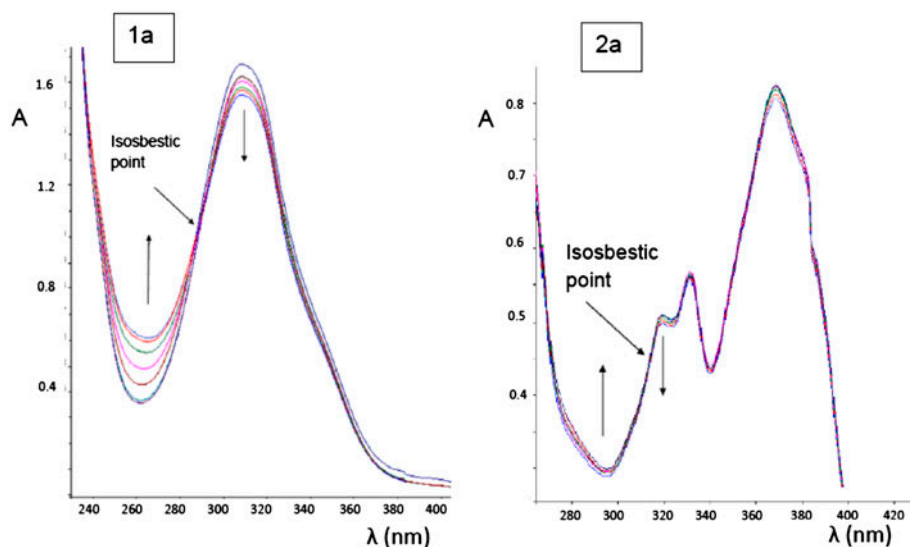


Figure 3. UV spectra of **1a** and **2a**. The arrows show the changes in absorbance upon increasing amounts of CT DNA.

contrast, K_b of $7.568 \times 10^5 \text{ M}^{-1}$ was observed for ligand **4**, whereas the lowest K_b was recorded for **3**. The ability to interact with DNA depends on the substituent on the aromatic ring, which is in the following order $\text{C}(\text{CH}_3)_3 > \text{OH} > \text{CH}_2\text{CH}=\text{CH}_2$, $\text{OCH}_3 > \text{C}_6\text{H}_5$. These groups facilitate intercalation between the complex and DNA because of changes in the planarity of complexes. The binding of the complexes to CT DNA resulted in isosbestic spectral changes with an isosbestic point at 297 nm in **1a**, **3a**, and **4a** and at 309 nm in **2a**.

3.3.2. Fluorescence spectroscopic studies. Fluorescence spectroscopic studies were performed on a spectrophotometer (Jasco FP-750) at 25 °C and in 6.3 mM Tris-HCl/50 mM NaCl buffer (pH 7). Fluorescence spectra (figure 4) show that the complexes have emission bands at 380 nm with hypochromism in **2a** and **4a**, and with hyperchromism in **1a** and **3a**. Complexes **1a** and **3a** have other emission bands at 525 and 500 nm, respectively, accompanied by hypochromism, which changed to hyperchromism at 380 nm because of the isosbestic spectral changes at 410 and 408 nm, respectively. No apparent shifts were observed

Table 3. DNA binding constants (K_b) of ligands and complexes.

Ligand	K_b (M^{-1})	Complex	K_b (M^{-1})
1	9.10×10^4	1a	2.14×10^5
2	4.68×10^4	2a	1.03×10^5
3	3.08×10^4	3a	2.24×10^5
4	7.56×10^5	4a	3.69×10^6

during the addition of CT DNA to the ligands or complexes. The fluorescence emission intensities show the complexes have strong interactions with DNA.

3.3.3. Viscometric studies. Interactions of the ligands and complexes with CT DNA were confirmed via viscometric studies. The intercalation of compounds in DNA increases viscosity because the DNA helix is lengthened as the base pairs are pushed apart [31]. Viscometric studies were performed by the addition of increasing amounts of CT DNA to the ligands and complexes at 37 °C in 6.3 mM Tris–HCl/50 mM NaCl buffer (pH 7). The results are shown in figure 5. The viscosity of solutions generally increases with the addition of CT DNA. These data support the results of spectrometric analysis.

3.4. DNA cleavage study

Agarose gel electrophoresis experiments that use pBR322 circular plasmid were performed for micro concentrations (1.0–6.0 μM) of ligands and complexes in aqueous 6.3 mM Tris–HCl/50 mM NaCl buffer (pH 7) in the presence of a fixed amount (4.5 μM) of 30% H_2O_2 as an oxidant. The solution was then incubated at 37 °C for 2 h. In figure 6, lane 4 of the agarose gel electrophoresis reveals that the ligands exhibit DNA cleavage with two forms of typical patterns; the fast migration form is related to the closed circular supercoiled form (SC, form I) and the slow migration form is related to the open circular relaxed form (OC, form II) [32]. Complexes **1** and **4** show only the SC form at 5 μM (lane 10). At 6 μM , both ligands can nick both strands of plasmid DNA, and this results in the linear form (form III) and the disappearance of SC form I (lane 6), whereas **2** and **3** denature the DNA. **3** can nick both DNA strands at 4.5 (lane 9) and 5 μM (lane 10), resulting in linear and SC forms and disappearance of the OC form. Complexes exhibit higher cleavage activity to plasmid DNA than their ligands. The complexes show SC, OC, and linear, and all of them denature plasmid DNA at 6 μM (lane 6). Complex **1a** shows the three forms at 4.5 μM (lane 9). However, at 5 μM (lane 10), the OC form disappears and only the SC and linear forms remain. Complex **2a** shows the SC and linear forms at 4 μM (lane 8), whereas the OC form accompanies the SC and linear forms at 4.5 μM (lane 9). At 5 μM , the SC form disappears

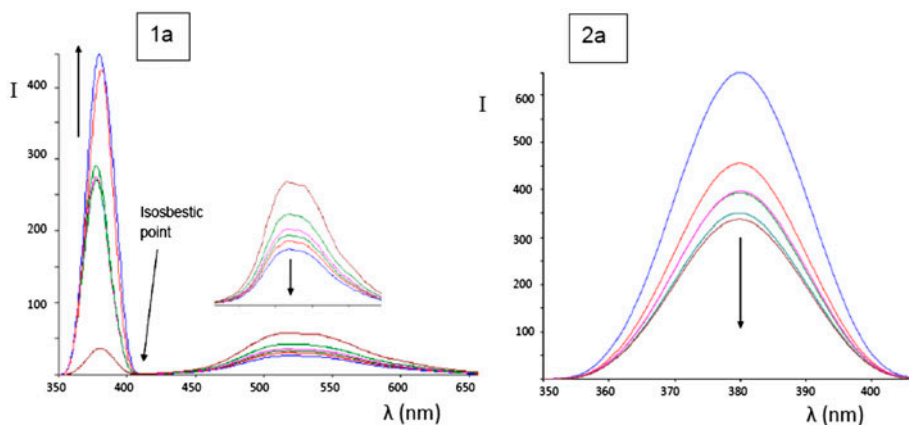


Figure 4. Fluorescence spectra of **1a** and **2a**. The arrows show the changes in fluorescence intensity upon increasing amounts of CT DNA.

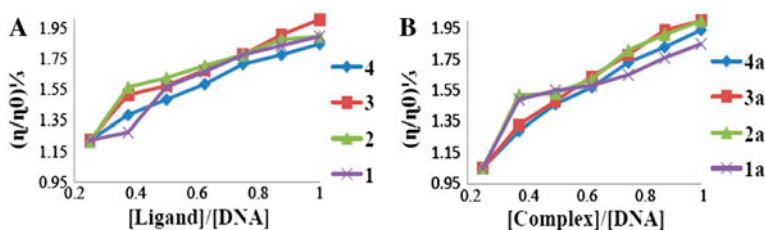


Figure 5. Viscometric results of ligands (A) and complexes (B) at 37 °C.

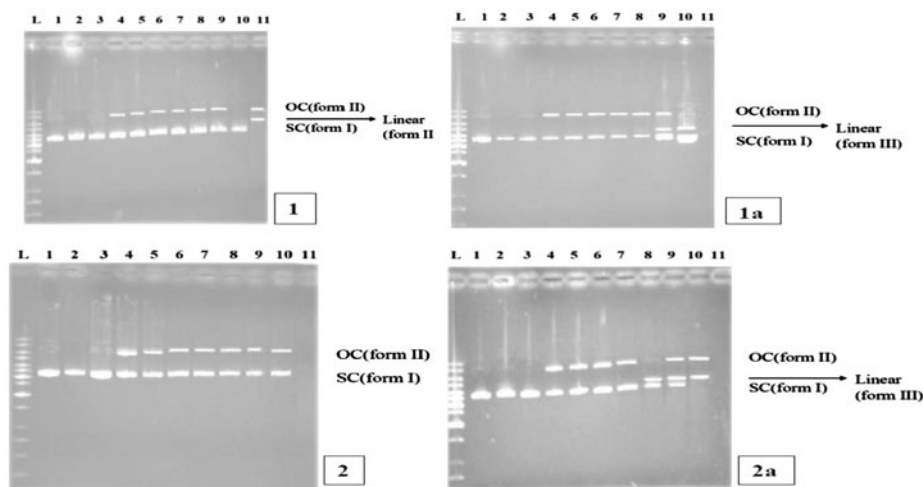


Figure 6. Agarose gel electrophoresis patterns of pBR322 (0.025 μM) with increasing concentrations (1.0–6.0 μM) of **1** and **2** and their complexes **1a** and **2a**.

and only the OC and linear forms remain. Complexes **3a** and **4a** show only SC and linear forms at 4 and 4.5 μM (lanes 8 and 9). At 5 μM (lane 10), **3a** shows only the linear form, whereas **4a** shows the OC and linear forms.

The agarose gel electrophoresis patterns show only the naturally occurring SC form (form I) for DNA control and buffer (lane 1), DNA and ligand or complexes (lane 2), and DNA, H_2O_2 , and buffer (lane 3). Thus, the ligands and complexes cleave DNA only in the presence of H_2O_2 as an oxidant (lanes 4–11) (4.5 μM) to different amounts of ligands and complexes (1–6 μM).

DNA cleavage enhanced in complexes over ligands indicates that these complexes may produce a hydroxyl radical from H_2O_2 . Generation of hydroxyl radicals from metal ions has been well reported [33, 34]. These free radicals share in the oxidation of deoxyribose moiety, followed by hydrolytic cleavage of the sugar-phosphate backbone [35].

3.5. Antitumor activity

Similar to the DNA binding and cleavage activities, the complexes demonstrated higher efficiency in antiproliferative activity than their respective ligands. Antiproliferation tests

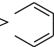
were performed *in vitro* on human colorectal cancer (HCT 116) cell line. The complexes exhibited more pronounced activity than the standard reference, 5-fluorouracil (median inhibitory concentration [IC₅₀] = 7.3 μM). The IC₅₀ values of the tested compounds (table 4) show that the order of antiproliferative efficiency was **4a** > **3a** > **1a** > **2a**, consistent with DNA binding, and confirm that complex activity is dependent on the substituent of the aromatic ring in the order (CH₃)₃ > OH > CH₂CH=CH₂, OCH₃ > . The inhibition activities of the complexes are listed in table 5, which shows that 100 μM **4a**, **1a**, **3a**, and **2a** is sufficient to inhibit 92.6, 69.4, 62.0, and 43.9% cell proliferation, respectively (figure 7). HCT 116 cell images after 48 h of treatment with the complexes is shown in

Table 4. IC₅₀ (μM) of **1a–4a**.

Complex	IC ₅₀ (μM)
1a	4.8
2a	6.7
3a	4.0
4a	1.6
5-FU	7.3

Table 5. % inhibition of cell proliferation by complexes using 3–100 μM.

Conc. (μM)	(% inhibition of cell proliferation)				
	1a	2a	3a	4a	5-FU
3	6.3	6.5	0.0	32.2	34
6	17.1	11.4	4.0	57.5	42
12	25.7	25.6	7.3	72.3	67
25	39.8	34.3	17.0	81.1	70
50	50.6	36.5	32.2	86.0	82
100	69.4	43.9	62.0	92.6	95

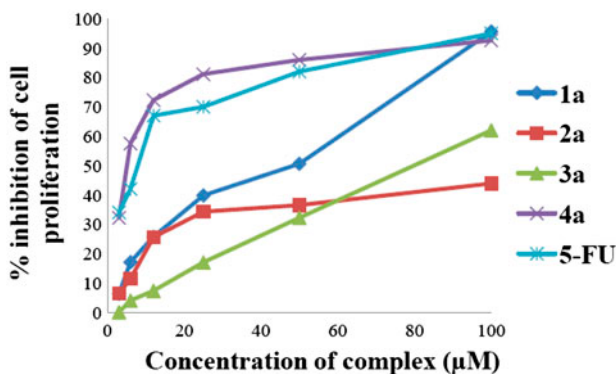


Figure 7. Cell proliferation inhibition by complexes in concentration range 3.0–100 μM using 5-FU as a reference.

Supplementary material (see online supplemental material at <http://dx.doi.org/10.1080/00958972.2014.893430>). These images were taken with inverted phase-contrast microscopy at $\times 200$ magnification and a digital camera at 48 h after treatment of the samples. The photomicrograph of the untreated (control) group showed aggressively growing cells with full confluence and a compact monolayer of HCT 116 cells. A close look at these images of untreated and treated cells shows strong cytotoxic effects of the complexes against HCT 116 cell line. Analysis of the photomicrographs shows that the complexes generally showed apoptotic features in the affected cells. The blabbing of the cell membrane, nuclear condensation, and vesicle formation in the treated cells indicate the unique characteristics of apoptosis.

4. Conclusion

The synthesis, structural description, and biological evaluation of molybdenum(VI) complexes **1a–4a** were studied. The complexes showed that the thiosemicarbazones coordinate to molybdenum as tridentate ONS donors. X-ray crystallography showed a distorted octahedral coordination. The complexes have high efficiency of CT DNA binding, as indicated by the high values of binding constant K_b , UV hypochromism of the absorption bands, fluorescence emission, and increase in viscosity because of the addition of CT DNA. The complexes also demonstrated a cleavage of plasmid pBR322 DNA with higher activity than their respective ligands.

The antiproliferative activities of the complexes were investigated against HCT 116 cell line in the order **4a** > **3a** > **1a** > **2a** corresponding to their IC_{50} values of 1.6, 4.0, 4.8, and 6.7 μ M, respectively.

Supplementary material

CCDC 885705, 969007, and 919582 contain the supplementary data for **1**, **3**, and **4**. CCDC 895506, 905156, 913192, and 913194 contain the supplementary data for **1a–4a**, respectively. These data can be obtained free of charge via http://www.ccdc.cam.ac.uk/data_request/cif.

Acknowledgements

We thank the Malaysian Government for a Research University Grant which partly supported this work. We also thank the University of Basrah, Iraq, for the study leave to Mouayed A. Hussein.

References

- [1] D.K. Johnson, T.B. Murphy, N.J. Rose, W.H. Goodwin, L. Pickart. *Inorg. Chim. Acta*, **67**, 159 (1982).
- [2] J.A. Craig, E.W. Harlan, B.S. Snyder, M.A. Whitener, R.H. Holm. *Inorg. Chem.*, **28**, 2082 (1989).
- [3] D. Sriram, P. Yogeewari, K. Madhu. *Bioorg. Med. Chem. Lett.*, **15**, 4502 (2004).
- [4] W.X. Hu, W. Zhou, C.N. Xia, X. Wen. *Bioorg. Med. Chem. Lett.*, **16**, 2213 (2006).
- [5] N.K. Ngan, K.M. Lo, C.S.R. Wong. *Polyhedron*, **33**, 235 (2012).
- [6] A.B. Beshir, S.K. Guchhait, J.A. Gascón, G. Fenteany. *Bioorg. Med. Chem. Lett.*, **18**, 498 (2008).

- [7] P. Kalaivani, R. Prabhakaran, P. Poornima, F. Dallemer, K. Vijayalakshmi, V. Vijaya Padma, K. Natarajan. *Organometallics*, **31**, 8323 (2010).
- [8] E.K. Efthimiadou, A. Karaliota, G. Psomas. *Polyhedron*, **27**, 349 (2008).
- [9] G. Pelosi. *Open Crystallogr. J.*, **3**, 16 (2010).
- [10] J.B. Waern, M.M. Harding. *Inorg. Chem.*, **43**, 206 (2004).
- [11] S. Quintal, J. Matos, I. Fonseca, V. Félix, M.G.B. Drew, N. Trindade, M. Meireles, M.J. Calhorda. *Inorg. Chim. Acta*, **361**, 1584 (2008).
- [12] V. Vrdoljak, I. Đilović, M. Rubčić, S. Kraljević Pavelić, M. Kralj, D. Matković-Čalogović, I. Piantanida, P. Novak, A. Rožman, M. Cindrić. *Eur. J. Med. Chem.*, **45**, 38 (2010).
- [13] D.C. Pryde. *J. Med. Chem.*, **53**, 8441 (2010).
- [14] R. Hille. *Arch. Biochem. Biophys.*, **433**, 107 (2005).
- [15] G. D'Errico, A. Di Salle, F. La Cara, M. Rossi, R. Cannio. *J. Bacteriol.*, **188**, 694 (2006).
- [16] D. Eierhoff, W.C. Tung, A. Hammerschmidt, B. Krebs. *Inorg. Chim. Acta*, **362**, 915 (2009).
- [17] E.B. Seena, M.R. Kurup. *Polyhedron*, **26**, 3595 (2007).
- [18] Z. Xiao, P.S. Donnelly, M. Zimmermann, A.G. Wedd. *Inorg. Chem.*, **47**, 4338 (2008).
- [19] M.E. Reichmann, S.A. Rice, C.A. Thomas, P.A. Doty. *J. Am. Chem. Soc.*, **76**, 3047 (1954).
- [20] S. Satyanarayana, J.C. Dabrowiak, J.B. Chaires. *Biochemistry*, **32**, 2573 (1993).
- [21] T. Mosmann. *J. Immunol. Methods*, **65**, 55 (1983).
- [22] I. Đilović, M. Rubčić, V. Vrdoljak, S. Pavelić, M. Kralj, I. Piantanida, M. Cindrić. *Bioorg. Med. Chem.*, **16**, 5189 (2008).
- [23] K.C. Agrawal, A.C. Sartorelli. *J. Pharm. Sci.*, **57**, 1948 (1968).
- [24] L. Coghi, A.M.M. Lanfredi, A. Tiripicchio. *J. Chem. Soc., Perkin Trans.*, **2**, 1808 (1972).
- [25] S. Tan, H. Yin, Z. Chen, X. Qian, Y. Xu. *Eur. J. Med. Chem.*, **62**, 130 (2013).
- [26] H. Xu, H. Deng, Q.L. Zhang, Y. Huang, J.Z. Liu, L.N. Ji. *Inorg. Chem. Commun.*, **6**, 766 (2003).
- [27] A. Oleksi, A.G. Blanco, R. Boer, I. Usón, J. Aymami, A. Rodger, M.J. Hannon, M. Coll. *Angew. Chem. Int. Ed.*, **45**, 1227 (2006).
- [28] R. Indumathy, M. Kanthimathi, T. Weyhermuller, B. Nair. *Polyhedron*, **27**, 3443 (2008).
- [29] N. Shahabadi, S. Kashanian, F. Darabi. *Eur. J. Med. Chem.*, **45**, 4239 (2010).
- [30] A. Wolfe, G.H. Shimer, T. Meehan. *Biochemistry*, **26**, 6392 (1987).
- [31] K.A. Meadows, F. Liu, J. Sou, B.P. Hudson. *Inorg. Chem.*, **32**, 2919 (1993).
- [32] E.J. Gao, M.C. Zhu, Y. Huang, L. Liu, H.-Y. Liu, F.-C. Liu, S. Ma. *Eur. J. Med. Chem.*, **45**, 1034 (2010).
- [33] C.X. Zhang, S.J. Lippard. *Curr. Opin. Chem. Biol.*, **7**, 481 (2003).
- [34] M.S. Babu, K. Reddy, P.G. Krishna. *Polyhedron*, **26**, 572 (2007).
- [35] W.K. Pogozelski, T.D. Tullius. *Chem. Rev.*, **98**, 1089 (1998).